however, its survival advantage is only 3.7 months [4]. New therapeutic targets are required to improve the survival of patients with HCC.

Signal transducer and activator of transcription 3 (STAT3) is an important molecule in tumor progression [5]. STAT3 activation occurs via phosphorylation and dimerization of tyrosine residue (Tyr705), leading to nuclear entry, DNA binding and gene transcription. STAT3 was regarded as a critical transcription activator for cell cycle- or cell survival-related genes. Bcl-XL is an antiapoptotic protein transcribed by STAT3 activation [6]. Some cytokines such as interleukin (IL)-6 or IL-10 activate STAT3 signaling via their receptors [7]. Constitutive activation of STAT3 has been demonstrated to contribute to tumorigenesis in breast cancer [8], colon cancer [9], lung cancer [10], pancreatic cancer [11], prostate cancer [12], and melanoma [13]. In human HCC, STAT3 phosphorylation was also detected and related to tumor progression [14], angiogenesis [15] and tumorigenesis [16]. The tumor microenvironment is closely associated with the growth of tumor cells, and tumor-associated macrophages play an important role in tumor progression [17]. Macrophages are major inflammatory cells that infiltrate tumors; several studies have shown that high infiltration of tumor-associated macrophages was associated with tumor progression and metastasis [17–20] and predicts poor prognosis in patients with HCC [21]. Tumor-associated macrophages activate STAT3 in ovarian cancer [22] and glioblastoma [23]. However, the correlation between tumor-associated macrophages and STAT3 activation of HCC tumor cells is unknown. Therefore, we examined STAT3 activation, cytokine expression and infiltration of tumor-associated macrophages in resected HCCs and analyzed their association with clinicopathological findings. Alterations in cell growth and migration by cytokine stimulation and STAT3 inhibitor were also analyzed in HCC cell lines.

Materials and Methods

Patients and Samples

One hundred and one available paraffin-embedded specimens from patients with HCC who underwent hepatectomy between January 1997 and December 2001 in our institute were selected by reviewing their pathology data. Any patients undergoing previous or noncurative surgery were excluded. After the surgery, monthly measurement of the serum α-fetoprotein (AFP) level was performed. In addition, ultrasonography and dynamic CT were performed every 3 months. The postoperative survival period or recurrence was entered into the database immediately when a patient died or if recurrence was strongly suspected on diagnostic imaging such as CT or magnetic resonance imaging.

This study conformed to the ethical guidelines of the 1975 Declaration of Helsinki and was approved by the ethics committees of Kyushu University Hospital (grant No. 21-117). Informed consent was obtained from each patient included in the study.

Immunohistochemistry

Sections of resected specimens were fixed in 10% buffered formalin, embedded in paraffin and stained by Envision+ system and DAB kit (Dako, Glostrup, Denmark). Immunohistochemical stains were performed with antibodies of phosphorylated STAT3 (pSTAT3; Tyr 705; D3A7, 1:50; Cell Signaling Technology), CD163 (10D6, 1:200; Novocastra), IL-6 (rabbit polyclonal, 1:1,000; Abcam), Ki-67 (MIB-1, 1:200; Dako), and Bcl-XL (rabbit polyclonal, 1:200; Santa Cruz Biotechnology, Santa Cruz, Calif., US). Sections were pretreated before being incubated with primary antibodies in a microwave oven at 99°C for 20 min for pSTAT3, CD163, IL-6 and Bcl-XL or in a pressure cooker for 25 min for Ki-67.

Each slide was stained in serial sections and examined by two pathologists (Y.M. and S.A.). In nuclear staining of pSTAT3 and Ki-67 and in cytoplasm staining of Bcl-XL, the percent positive cells was estimated by count of 1,000 tumor cells in most staining areas (hot spots). Staining of CD163, a marker of tumor-associated macrophages [19, 22–25], and IL-6 was evaluated by estimating the total counts of cytoplasm or membrane at 3 high-power fields. The mean of nuclear pSTAT3-positive cells in HCCs was 10.7% (range 0–82.0), and pSTAT3 stain was classified into a positive (≥10.7% of tumor cell nuclei) and a negative group (<10.7% of tumor nuclei). Furthermore, in the cases of the pSTAT3-positive group (n = 36), the CD163-positive cells were counted separately in areas of pSTAT3-positive and pSTAT3-negative HCC cells.

For double staining of IL-6 and CD163, HCC specimens were boiled in 10 mM citrate buffer (pH 6.0) for 20 min and incubated with IL-6 primary antibody (1:1,000) at room temperature for 15 min. The sections were washed three times and incubated with anti-rabbit horseradish peroxidase-conjugated polymer at room temperature for 45 min; IL-6 was visualized by DAB kit. Next, the sections were boiled in 10 mM citrate buffer (pH 6.0) for 10 min, incubated with CD163 primary antibody (1:200) for 90 min and incubated with anti-mouse alkaline phosphatase-conjugated polymer at room temperature for 45 min. CD163 of the sections was visualized by New Fuchsin Substrate kit (Nichirei, Tokyo, Japan).

Cell Culture

Human HCC cell lines PLC/PRF/5 and Huh7 were obtained from Riken Bioresource Center, Tsukuba, Japan, and cultured in Dulbecco's modified Eagle's medium (DMEM) supplemented with 1 or 10% fetal bovine serum (FBS). PLC/PRF/5 and Huh7 cells were maintained in DMEM containing 1% FBS for 24 h prior to IL-6 (Peprotech, Rocky Hill, N.J., USA) stimulation. All in vitro experiments were done in triplicate.

Immunoblotting

Cellular proteins were solubilized in lysis buffer containing protease inhibitor and phosphatase inhibitor 30 min after stimulation with IL-6 (20 μg/ml). Equal amounts of protein were separated by SDS-PAGE and then transferred to the polyvinylidene fluoride membrane. Following blocking in Tris buffer containing 2% BSA, the membrane was stained with 1:1,000 dilution of anti-STAT3 (Cell Signaling Technology, Danvers, Mass., USA) and anti-pSTAT3 (Cell Signaling Technology) antibodies, then

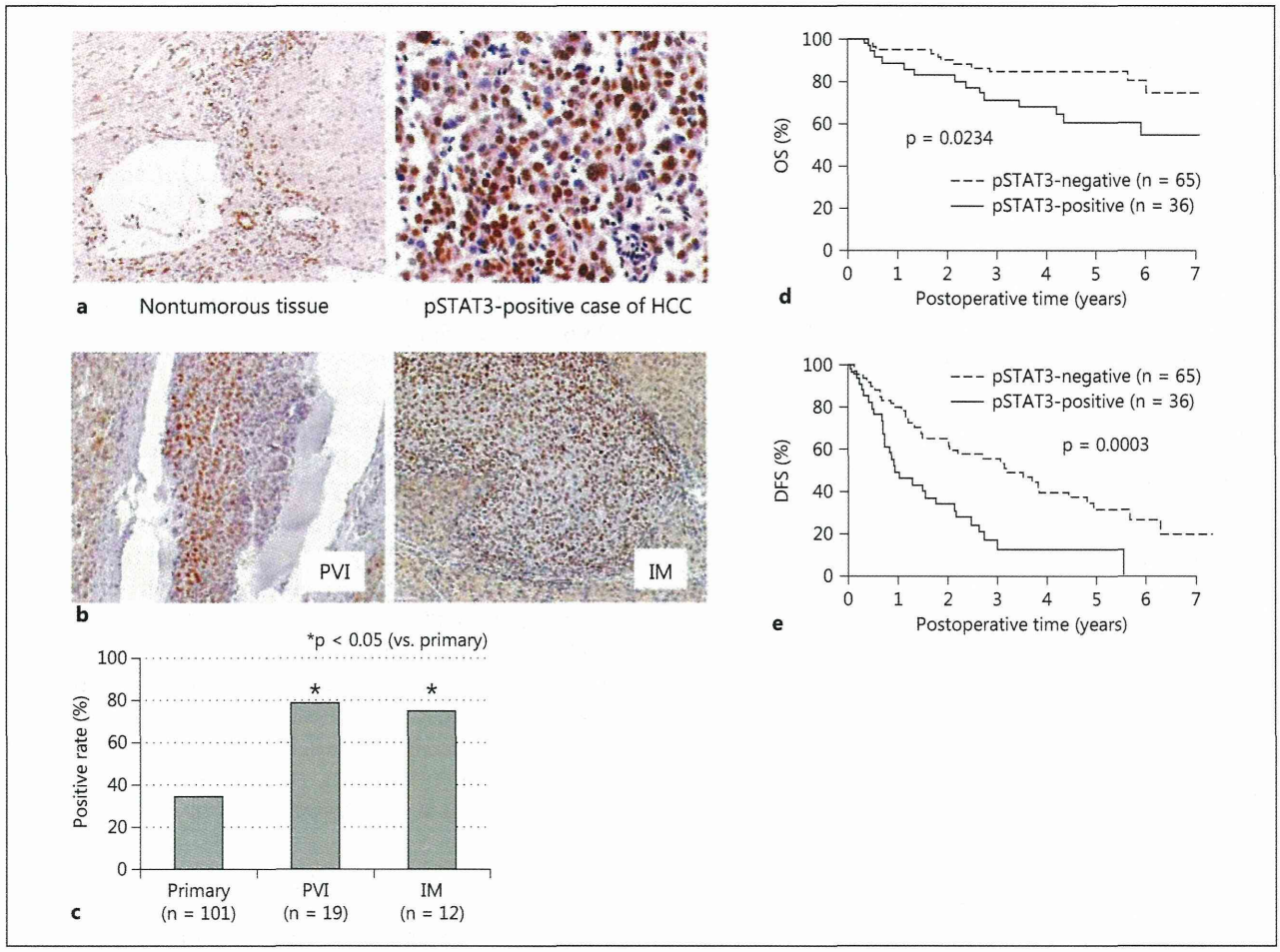

Fig. 1. Immunohistochemical staining of pSTAT3 in HCC. **a** pSTAT3 was expressed in the nucleus. In nontumorous tissue, endothelial cells, bile duct epithelial cells and inflammatory cells were stained by pSTAT3 (left panel). ×100. HCC cells were also stained (82.2%, right panel). ×100. **b** Tumor cells of PVI and IM stained by pSTAT3. ×200. **c** Comparison of pSTAT3 staining in primary HCC, tumor cells of PVI and IM. pSTAT3 staining was significantly prominent in tumor cells of PVI and IM compared with primary HCC ($p < 0.05$). **d**, **e** pSTAT3 expression correlated with poor prognosis. OS (**d**) and DFS (**e**) curves for pSTAT3-positive and pSTAT3-negative groups in patients with HCC (**d**, $p = 0.0234$; **e**, $p = 0.0003$; log-rank test).

washed and incubated with horseradish peroxidase-conjugated secondary antibody (Cell Signaling Technology). Bands were visualized by the enhanced chemiluminescence system (GE Healthcare, UK).

Cell Growth Assay

PLC/PRF/5 and Huh7 cells were seeded at a density of 5×10^4 cells/24-well plates and maintained in conditioned medium for 24 h before stimulation. Viable cells were counted by trypan blue stain 48 h after stimulation with IL-6 (25 ng/ml).

Wound-Healing Assay

PLC/PRF/5 and Huh7 cells were seeded at a density of 5×10^4 cells/6-well plates. Approximately 24 h later, when the cells were 100% confluent, a sterile 100-μl pipette tip was used to longitudinally scratch a constant-diameter strip in the confluent monolayer. The medium and cell debris were aspirated away and replaced by 2 ml of fresh DMEM containing 1% FBS with or without IL-6 (25 ng/ml). Photographs were taken at 0 and 48 h after wounding by phase-contrast microscopy. For statistical analysis, three randomly selected points along each wound were marked, and the horizontal distance between the migrating cells and the initial wound was measured 48 h later.

Inhibition of STAT3

In both cell growth and wound-healing assays, PLC/PRF/5 and Huh7 cells were cultured in DMEM containing 1% FBS and IL-6 (25 ng/ml) with or without 100 nM S3I-201 (NSC 74859; Santa Cruz Biotechnology). S3I-201 was treated 30 min before IL-6 stimulation. DMSO was used for control.

Table 1. Comparison of pSTAT3 expression and clinicopathological findings

pSTAT3 expression	pSTAT3 negative (n = 65)	pSTAT3 positive (n = 36)	p value
Clinical features			
Sex, male/female	55/10	26/10	0.0849
Age, years	63.9±7.3	63.6±9.5	0.8726
HBsAg, +/–	14/51	8/28	0.9922
HCV Ab, +/–	42/23	23/13	0.9798
Cirrhosis	22/43	14/22	0.4990
AFP, ng/ml	852.4±308†	20,673.4±11,688†	0.0276*
DCP, mAU/ml	2,798.2±1,179.1†	6,278.4±3,184.7†	0.2217
Pathological features			
Tumor size, cm	3.7±2.2	5.1±3.2	0.0092*
Differentiation, poor/well and moderate	19/46	16/20	0.1253
Capsule formation	41/24	26/10	0.4619
Infiltration to the capsule	33/32	23/13	0.1681
Portal venous invasion, +/–	30/35	24/12	0.0687
Hepatic venous invasion, +/–	15/50	12/24	0.3031
Intrahepatic metastasis, +/–	18/47	18/18	0.0214*
MIB-1 LI, %	3.5±0.5	10.2±2.2	0.0002*
Bcl-XL, %	13.0±1.5	25.2±2.0	0.0001*

HBsAg = Hepatitis B surface antigen; HCV Ab = hepatitis C virus antibody; DCP = des-γ-carboxy prothorombin. * $p < 0.05$.

Statistical Analysis

Statistical analysis was carried out using Microsoft Excel software and JMP software (SAS Institute, Cary, N.C., USA). Comparison between pSTAT3 staining and clinicopathological findings or staining of other antibodies was evaluated by Pearson's χ^2, Fisher's exact tests and the Mann-Whitney U test. Patient survival analysis including overall survival (OS) and disease-free survival (DFS) was calculated by the Kaplan-Meier method; differences were evaluated by the log-rank test. For multivariate analysis, the Cox proportional hazard model was used. Two-sided Student's t test was applied for analysis of in vitro data. Statistical analyses were considered significant at a p value <0.05.

Results

pSTAT3 Expression in Clinical Samples

pSTAT3 was stained in the nuclei of HCC cells, normal endothelial cells, some bile duct epithelial cells and inflammatory cells. pSTAT3 nuclear staining in HCC cells is displayed in figure 1a. The mean percentage of nuclear pSTAT3-positive cells in HCCs was 10.7% (range 0–82.0). The number of pSTAT3-positive and pSTAT3-negative samples was 36 and 65, respectively. We also examined pSTAT3 staining at the lesions of 19 portal venous invasions (PVIs) and 12 intrahepatic metastases (IMs) in 101 cases. Fifteen of 19 PVIs (78.9%) and 9 of 12 (75.0%) IMs were defined as pSTAT3-positive cases (fig. 1b). Positive rates in both lesions were significantly higher than those in the primary lesions (35.6%; $p < 0.05$; fig. 1c).

Comparison of pSTAT3 Expression and Clinicopathological Findings

A comparison of clinicopathological findings in pSTAT3-positive and pSTAT3-negative groups is summarized in table 1. The pSTAT3-positive group showed higher AFP ($p = 0.0276$), larger tumor size ($p = 0.0092$), more frequent IMs ($p = 0.0214$), a higher Ki-67 labeling index (LI; $p = 0.0002$), and more Bcl-XL-positive cells ($p = 0.0001$) than the pSTAT3-negative group, whereas no significant differences were noted with respect to sex, age, infection of hepatitis viruses, liver cirrhosis, PIVKA II (proteins induced by vitamin K absence or antagonist II), histological differentiation, capsule formation, infiltration to the capsule, and vessel invasion.

Survival Analysis after Surgery

The median follow-up period was 1,391 days (range 36–3,289). pSTAT3 expression was significantly correlated with OS and DFS ($p = 0.0234$ and 0.0003, respectively; fig. 1d, e). Univariate analyses indicated that high AFP (>100 ng/ml), large tumor size (>5 cm), PVIs and IMs were prognostic factors for OS and male sex, hepatitis C virus infection, high AFP (>100 ng/ml) and IMs for DFS (table 2). Multivariate proportional hazard models revealed that high AFP and IMs were independent prognostic factors for OS and pSTAT3 expression and high AFP for DFS (table 2).

Tumor-Associated Macrophage Localization and pSTAT3 Expression of HCCs

CD163-positive cells were localized around the pSTAT3-positive HCC cells (fig. 2a). Figure 2b shows the boxplots of CD163-positive cells (mean ± SD: pSTAT3-negative group, 28.5 ± 15.4; pSTAT3-positive group, 42.6 ± 26.6). The pSTAT3-positive group (n = 36) showed statistically higher CD163-positive cells ($p = 0.0013$; fig. 2b) than the pSTAT3-negative group (n = 65). Furthermore, we analyzed the localization of CD163-posi-

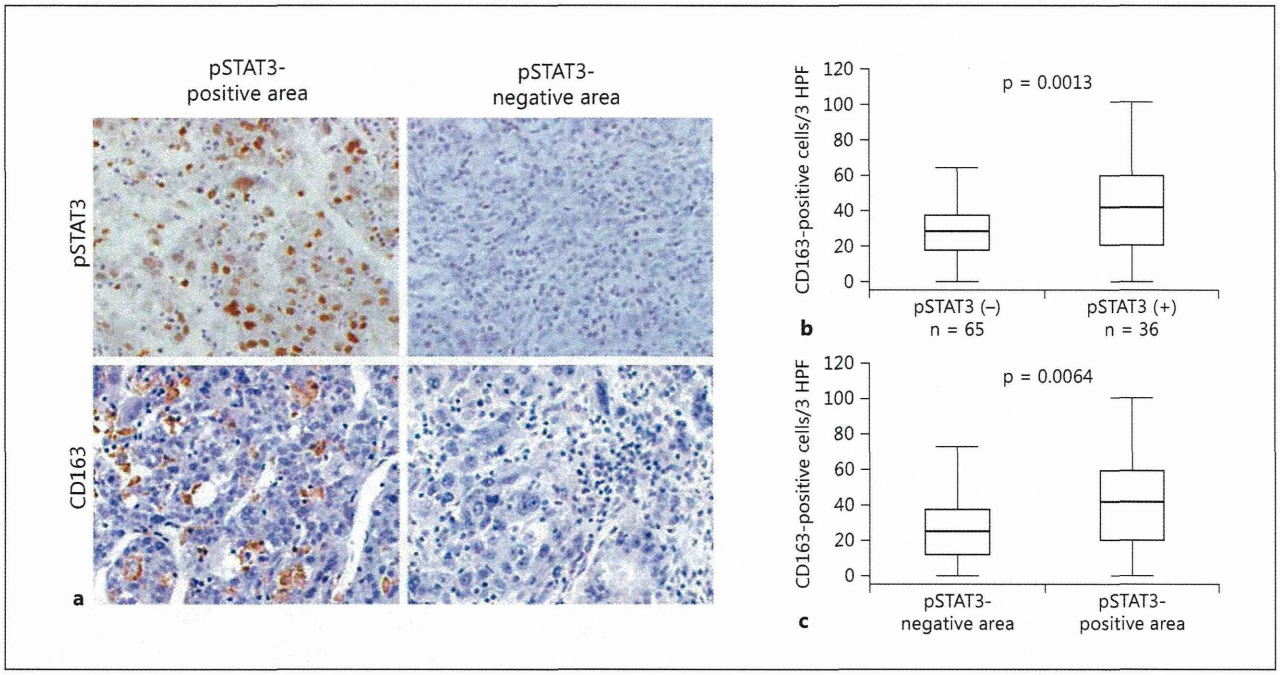

Fig. 2. Tumor-associated macrophages correlated with pSTAT3 expression in HCC. **a** Immunohistochemical staining of pSTAT3 and CD163 in the pSTAT3-positive and pSTAT3-negative area. ×200. **b** Counts of CD163-positive cells between pSTAT3-positve and pSTAT3-negative groups. **c** Counts of CD163-positive cells in areas of pSTAT3-positive and pSTAT3-negative HCC cells existed in the pSTAT3-positive group. HPF = High-power field.

Table 2. Survival analysis after surgery

Variable	Univariate analysis of OS	Multivariate analysis of OS		
	p value	hazard ratio	95% CI	p value
pSTAT3 positive	0.0234*	1.104	0.465–2.683	0.8236
AFP >100 ng/ml	0.0005*	2.968	1.294–7.026	0.0103*
Tumor size >5 cm	0.0246*	1.489	0.610–3.578	0.3755
Portal venous invasion	0.0422*	1.568	0.629–4.1265	0.3367
Intrahepatic metastasis	0.0022*	2.668	1.186–6.194	0.0177*
Variable	Univariate analysis of DFS	Multivariate analysis of DFS		
	p value	hazard ratio	95% CI	p value
pSTAT3 positive	0.0003*	1.851	1.066–3.201	0.0288*
Sex, male	0.0267*	0.978	0.515–1.790	0.9431
HCV Ab (+)	0.0158*	1.672	0.948–3.096	0.0767
AFP >100 ng/ml	0.0002*	2.070	1.218–3.476	0.0076*
Intrahepatic metastasis	0.0012*	1.702	0.964–3.012	0.0664

CI = Confidence interval; HCV Ab = hepatitis C virus antibody. * $p < 0.05$.

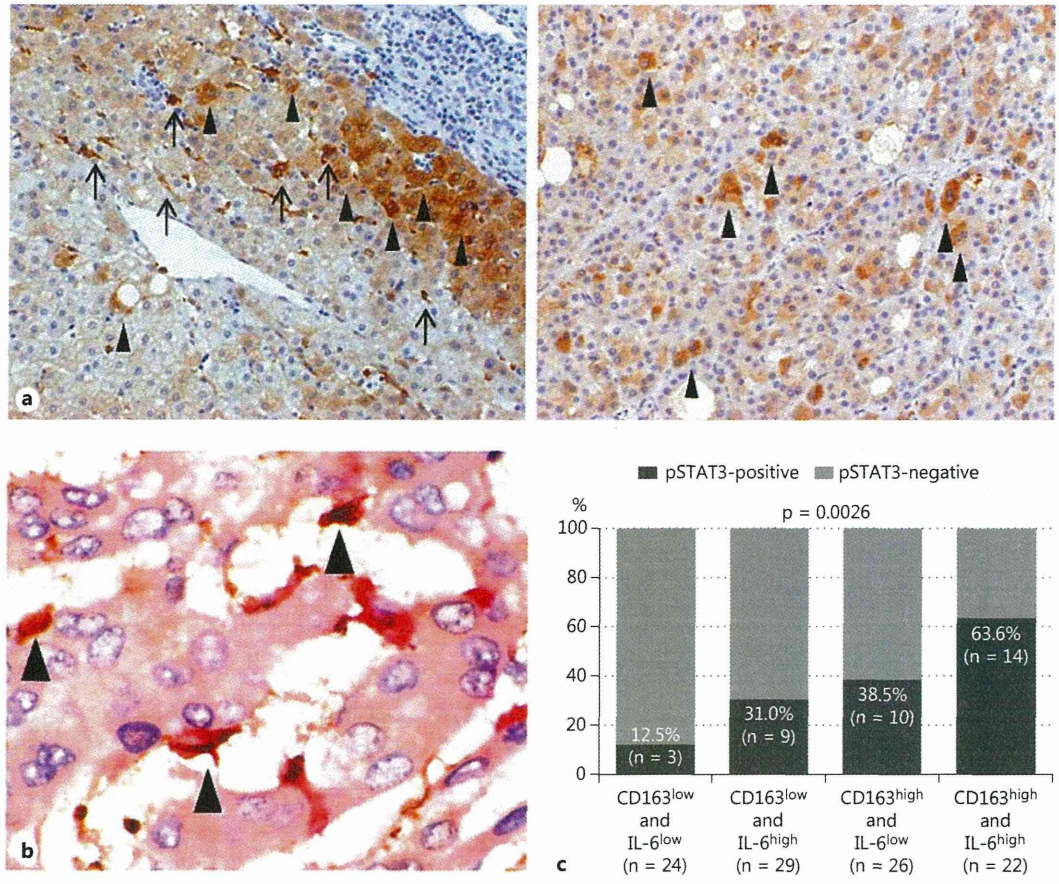

Color version available online

Fig. 3. Tumor-associated macrophages expressed IL-6. **a** Immunohistochemical staining of IL-6 in HCC. ×200. Not only macrophages (arrows, left panel) but also some hepatocytes (arrowheads, left panel) and some tumor cells (arrowheads, right panel) showed immunoreactivities for IL-6. **b** Double staining of IL-6 (red) and CD163 (brown). ×400. Double-positive cells (arrowheads) were frequently seen in the tumor. **c** Correlation between pSTAT3-positive and IL-6/CD163-positive staining.

tive cells in areas where pSTAT3-positive and pSTAT3-negative HCC cells existed in the pSTAT3-positive group (n = 36), and figure 2c shows the boxplots of the analyses (mean ± SD: pSTAT3-negative area, 27.7 ± 17.9; pSTAT3-positive area, 42.6 ± 26.6). In the pSTAT3-positive group, CD163-positive cells in areas where pSTAT3-positive HCC cells existed were statistically higher than in those where pSTAT3-negative HCC cells existed (p = 0.0064; fig. 2c).

Cytokine Expression of Macrophages

IL-6 was stained in some macrophages, HCC cells and normal hepatocytes (fig. 3a). According to the double staining of CD163 and IL-6, CD163-positive cells (tumor-associated macrophages) expressed IL-6 (fig. 3b). We divided them into two by the median values of positive macrophages of IL-6 and CD163, and thereby classified the 101 cases into four groups such as $CD163^{low}$ and $IL\text{-}6^{low}$, $CD163^{low}$ and $IL\text{-}6^{high}$, $CD163^{high}$ and $IL\text{-}6^{low}$, and $CD163^{high}$ and $IL\text{-}6^{high}$. HCCs containing high infiltration of IL-6- and CD163-positive macrophages exhibited a significantly higher rate of positive staining for pSTAT3 (fig. 3c).

IL-6 Stimulates Cell Proliferation and Migration of Human HCC Cell Lines

IL-6 stimulation increased the levels of pSTAT3 in both PLC/PRF/5 and Huh7 HCC cell lines (fig. 4a). IL-6 stimulation resulted in higher proliferation (fig. 4b) and greater migration distance (fig. 4c) versus control. S3I-

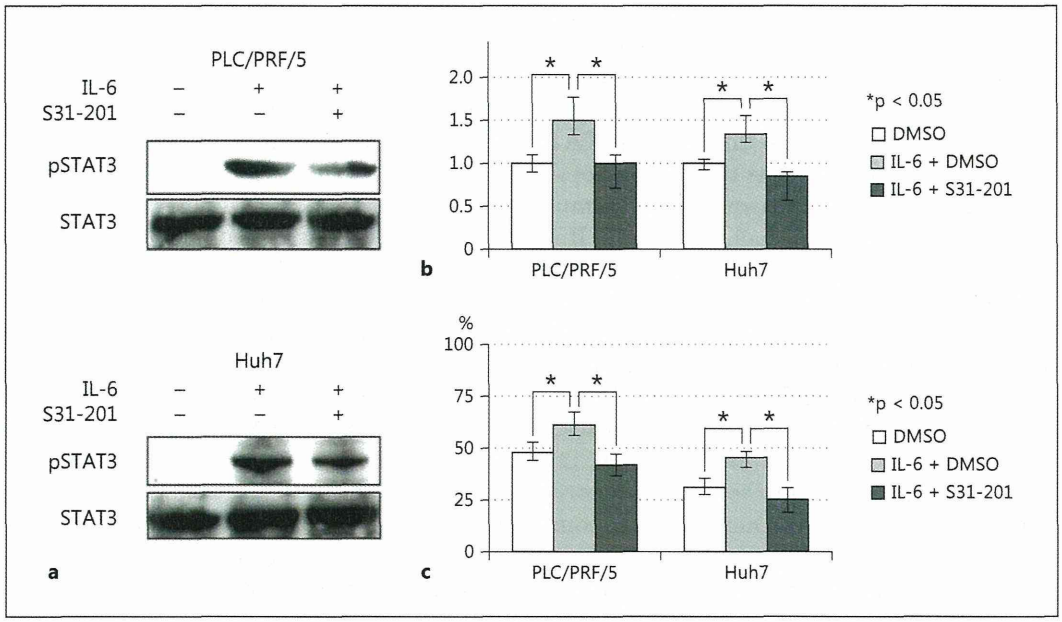

Fig. 4. IL-6 stimulation activated STAT3 signaling and promoted cell proliferation and migration in HCC cell lines. **a** PLC/PRF/5 (upper panel) and Huh7 (lower panel) were treated with 25 ng/ml IL-6 for 30 min. **b** PLC/PRF/5 and Huh7 were cultured with 25 ng/ml IL-6, 100 nM S3I-201 and conditioned medium (1% FBS); cell proliferation was evaluated 48 h after IL-6 stimulation. Control set at 1. **c** PLC/PRF/5 and Huh7 were cultured with 25 ng/ml IL-6, 100 nM S3I-201 and conditioned medium (1% FBS), and wound-healing assay was evaluated 48 h thereafter.

201, a STAT3 inhibitor, inhibited IL-6-induced STAT3 phosphorylation (fig. 4a) and decreased proliferation and migration of HCC cell lines (fig. 4b, c).

Discussion

Our results suggest that macrophage infiltration into HCC tissue stimulates tumor cells via STAT3 signaling. In the present study, pSTAT3-positive HCCs show malignant behavior and confer poor prognosis because of their high abilities of cell proliferation and migration. We found that high pSTAT3 expression was significantly correlated with larger tumor size, higher Ki-67 LI, higher Bcl-XL expression and greater frequency of IMs, and higher pSTAT3 expression was observed in the lesions of IMs and PVIs than in the primary lesions. STAT3 activation upregulates cell cycle-related, antiapoptotic and invasion genes [8–13, 26, 27]. In our results, large tumor size and high Ki-67 LI indicated cell cycle progression, high Bcl-XL expression indicated antiapoptotic function, and frequent IMs indicated invasive capacity. Furthermore, high pSTAT3 expression in the lesions of IMs and PVIs suggests that the tumor cells with STAT3 activation in the primary lesions tended to invade the vessels and metastasize to the other liver sites. Xie et al. [26, 27] reported that activated STAT3 regulated tumor invasion of melanoma cells by regulating the gene transcription of matrix metalloproteinase 2. These results suggest that pSTAT3 expression plays an important role for cell survival and migration in HCC, consistent with previous studies in HCC [14, 17, 28, 29] and other tumors [5, 8–12, 26, 27, 30].

In recent years, it has been recognized that the balance between tumor immunity and tumor progression is important [31]. The present study revealed that tumor-associated macrophages are important for pSTAT3 expression of tumor cells. First, CD163-positive cells around pSTAT3-positive HCC cells were statistically more prevalent than around pSTAT3-negative HCC cells. Some of the CD163-positive cells expressed IL-6 in HCC tissue, and STAT3 was phosphorylated by IL-6 stimulation in vitro. These results suggest that tumor-associated macrophages can activate HCC cells via STAT3 signaling by IL-6 expression. However, CD-163-positive cells were detected not only in the pSTAT3-negative tumor area but

also in the pSTAT3-positive tumor area and in noncancerous liver tissue. IL-6-secreting tumor-associated macrophages may be part of the CD163-positive cells, and the CD163-positive cells in the pSTAT3-positive tumor area were more stained by IL-6 than in the pSTAT3-negative tumor area and normal liver tissue (data not shown). Tumor-associated macrophages express immunosuppressive cytokines including IL-4, IL-6, IL-10, IL-17, and IL-23 [32, 33]. These cytokines activate immunosuppressive inflammatory cells such as other tumor-associated macrophages, helper T cells and regulatory T cells and suppress antitumor inflammatory cells such as lymphocytes, natural killer cells and dendritic cells [34–36]. Kuang et al. [32] showed that tumor-associated macrophages expressed IL-6 in vitro, whereas Ding et al. [21] reported that tumor-associated macrophage was correlated with poor prognosis in HCC. Our results are consistent with these previous reports.

Both proliferation and migration of PLC/RPF/5 and Huh7 were increased following IL-6 stimulation and STAT3 phosphorylation. On the other hand, IL-6 was expressed in not only macrophages but also in HCC cells. STAT3 can be activated through autocrine signaling in HCC cells; moreover, other cytokines and growth factors might activate STAT3 of tumor cells [22–24]. It is very difficult to exclude activation of STAT3 by the autocrine manner. In our data, STAT3 activation of HCC cells was not correlated with surrounding IL-6-positive normal hepatocytes and HCC cells but it was correlated with the infiltration of CD-163-positive cells (fig. 2). Thus, we thought that the IL-6 secretion of tumor-associated macrophages is more important for STAT3 activation of HCC cells than the IL-6 secretion of other cells.

Recently, STAT3 phosphorylation inhibitors such as S3I-201 have been investigated in vitro and in vivo [28–30]. Avella et al. [37] reported that STAT3 can be one of the targets of chemoimmunotherapies. In our study, S3I-201 inhibited IL-6-induced STAT3 phosphorylation in vitro and decreased cell proliferation and migration. The inhibition of tumor-associated macrophages as therapeutic strategy of malignancy has been investigated, too [38–41]. Therefore, it is very important to suppress tumor-associated macrophage activation and STAT3 signaling in the treatment of HCC. Furthermore, tumor-associated macrophage activation requires STAT3 signaling [22]. We consider that the STAT3 inhibitor may suppress STAT3 activation in both tumor cells and tumor-associated macrophages, release antitumor immune systems from suppression by tumor-associated macrophages and thereby control tumor progression of HCC. Therefore, STAT3 signaling is a feasible therapeutic target for HCC.

In conclusion, STAT3 activation is one of the prognostic factors in HCC. Tumor-associated macrophage expresses IL-6 and can activate STAT3 signaling of HCC cells, resulting in their cell proliferation, antiapoptosis and migration. In the future, HCC may be suppressed by inhibition of STAT3 signaling of tumor cells and tumor-associated macrophages.

Disclosure Statement

The authors have no conflicts of interest.

References

1 Llovet JM, Burroughs A, Bruix J: Hepatocellular carcinoma. Lancet 2003;362:1907–1917.
2 Shirabe K, Kanematsu T, Matumata T, Adachi E, Akazawa K, Sugimachi K: Factors linked to early recurrence of small hepatocellular carcioma after hepatectomy: univariate and multivariate analyses. Hepatology 1991; 14:802–805.
3 Taura K, Ikai I, Hatano E, Fujii H, Uyama N, Shimahara Y: Implication of frequent local ablation therapy for intrahepatic recurrence in prolonged survival of patients with hepatocellular carcinoma undergoing hepatic resection: an analysis of 610 patients over 16 years old. Ann Surg 2006;244:265–273.
4 Llovet JM, Ricci S, Mazzaferro V, Hilgard P, Gane E, Blanc JF, de Oliveira AC, Santoro A, Raoul JL, Forner A, Schwartz M, Porta C, Zeuzem S, Bolondi L, Greten TF, Galle PR, Seitz JF, Borbath I, Häussinger D, Giannaris T, Shan M, Moscovici M, Voliotis D, Bruix J, SHARP Investigators Study Group: Sorafenib in advanced hepatocellular carcinoma. N Engl J Med 2008;359:378–390.
5 Bromberg JF, Wrzeszczynska MH, Devgan G, Zhao Y, Pestell RG, Albanese C, Darnell JE Jr: Stat3 as an oncogene. Cell 1999;98:295–303.
6 Al Zaid Siddiquee K, Turkson J: STAT3 as a target for inducing apoptosis in solid and hematological tumors. Cell Res 2008;18:254–267.
7 Murray PJ: The JAK-STAT signaling pathway: input and output integration. J Immunol 2007;178:2623–2629.
8 Berishaj M, Gao SP, Ahmed S, Leslie K, Al-Ahmadie H, Gerald WL, Bornmann W, Bromberg JF: Stat3 is tyrosine-phosphorylated through the interleukin-6/glycoprotein 130/Janus kinase pathway in breast cancer. Breast Cancer Res 2007;9:R32.

9 Lin Q, Lai R, Chirieac LR, Li C, Thomazy VA, Grammatikakis I, Rassidakis GZ, Zhang W, Fujio Y, Kunisada K, Hamilton SR, Amin HM: Constitutive activation of JAK3/STAT3 in colon carcinoma tumors and cell lines: inhibition of JAK3/STAT3 signaling induces apoptosis and cell cycle arrest of colon carcinoma cells. Am J Pathol 2005;167:969–980.
10 Song L, Turkson J, Karras JG, Jove R, Haura EB: Activation of Stat3 by receptor tyrosine kinases and cytokines regulates survival in human non-small cell carcinoma cells. Oncogene 2003;22:4150–4165.
11 Greten FR, Weber CK, Greten TF, Schneider G, Wagner M, Adler G, Schmid RM: Stat3 and NF-kappaB activation prevents apoptosis in pancreatic carcinogenesis. Gastroenterology 2002;123:2052–2063.
12 Ni Z, Lou W, Leman ES, Gao AC: Inhibition of constitutively activated Stat3 signaling pathway suppresses growth of prostate cancer cells. Cancer Res 2000;60:1225–1228.
13 Kreis S, Munz GA, Haan S, Heinrich PC, Behrmann I: Cell density dependent increase of constitutive signal transducers and activators of transcription 3 activity in melanoma cells is mediated by Janus kinases. Mol Cancer Res 2007;5:1331–1341.
14 Rajendran P, Ong TH, Chen L, Li F, Shanmugam MK, Vali S, Abbasi T, Kapoor S, Sharma A, Kumar AP, Hui KM, Sethi G: Suppression of signal transducer and activator of transcription 3 activation by butein inhibits growth of human hepatocellular carcinoma in vivo. Clin Cancer Res 2011;17:1425–1439.
15 Yang SF, Wang SN, Wu CF, Yeh YT, Chai CY, Chunag SC, Sheen MC, Lee KT: Altered p-STAT3 (Tyr705) expression is associated with histological grading and intratumour microvessel density in hepatocellular carcinoma. J Clin Pathol 2007;60:642–648.
16 Ogata H, Kobayashi T, Chinen T, Takaki H, Sanada T, Minoda Y, Koga K, Takaesu G, Maehara Y, Iida M, Yoshimura A: Deletion of the SOCS3 gene in liver parenchymal cells promotes hepatitis-induced hepatocarcinogenesis. Gastroenterology 2006;131:179–193.
17 Pollard JW: Tumour-educated macrophages promote tumour progression and metastasis. Nat Rev Cancer 2004;4:71–78.
18 Lewis CE, Pollard JW: Distinct role of macrophages in different tumor microenvironments. Cancer Res 2006;66:605–612.
19 Hasita H, Komohara Y, Okabe H, Masuda T, Ohnishi K, Lei XF, Beppu T, Baba H, Takeya M: Significance of alternatively activated macrophages in patients with intrahepatic cholangiocarcinoma. Cancer Sci 2010;101:1913–1919.
20 Siveen KS, Kuttan G: Role of macrophages in tumor progression. Immunol Letter 2009;123:97–102.
21 Ding T, Xu J, Wang F, Shi M, Zhang Y, Li SP, Zheng L: High tumor-infiltrating macrophage density predicts poor prognosis in patients with primary hepatocellular carcinoma after resection. Hum Pathol 2009;40:381–389.
22 Fujiwara Y, Komohara Y, Ikeda T, Takeya M: Corosolic acid inhibits glioblastoma cell proliferation by suppressing the activation of signal transducer and activator of transcription-3 and nuclear factor-kappa B in tumor cells and tumor-associated macrophages. Cancer Sci 2011;102:206–211.
23 Takaishi K, Komohara Y, Tashiro H, Ohtake H, Nakagawa T, Katabuchi H, Takeya M: Involvement of M2-polarized macrophages in the ascites from advanced epithelial ovarian carcinoma in tumor progression via Stat3 activation. Cancer Sci 2010;101:2128–2136.
24 Domínguez-Soto A, Sierra-Filardi E, Puig-Kröger A, Pérez-Maceda B, Gómez-Aguado F, Corcuera MT, Sánchez-Mateos P, Corbí AL: Dendritic cell-specific ICAM-3-grabbing nonintegrin expression on M2-polarized and tumor-associated macrophages is macrophage-CSF dependent and enhanced by tumor-derived IL-6 and IL-10. J Immunol 2011;186:2192–2200.
25 Komohara Y, Ohnishi K, Kuratsu J, Takeya M: Possible involvement of the M2 anti-inflammatory macrophage phenotype in growth of human gliomas. J Pathol 2008;216:15–24.
26 Xie TX, Wei D, Liu M, Gao AC, Ali-Osman F, Sawaya R, Huang S: Stat3 activation regulates the expression of matrix metalloproteinase-2 and tumor invasion and metastasis. Oncogene 2004;23:3550–3560.
27 Xie TX, Huang FJ, Aldape KD, Kang SH, Liu M, Gershenwald JE, Xie K, Sawaya R, Huang S: Activation of Stat3 in human melanoma promotes brain metastasis. Cancer Res 2006;66:3188–3196.
28 Lin L, Amin R, Gallicano GI, Glasgow E, Jogunoori W, Jessup JM, Zasloff M, Marshall JL, Shetty K, Johnson L, Mishra L, He AR: The STAT3 inhibitor NSC 74859 is effective in hepatocellular cancers with disrupted TGF-beta signaling. Oncogene 2009;28:961–972.
29 Choudhari SR, Khan MA, Harris G, Picker D, Jacob GS, Block T, Shailubhai K: Deactivation of Akt and STAT3 signalling promotes apoptosis, inhibits proliferation, and enhances the sensitivity of hepatocellular carcinoma cells to an anticancer agent, Atiprimod. Mol Cancer Ther 2007;6:112–121.
30 Lin L, Hutzen B, Zuo M, Ball S, Deangelis S, Foust E, Pandit B, Ihnat MA, Shenoy SS, Kulp S, Li PK, Li C, Fuchs J, Lin J: Novel STAT3 phosphorylation inhibitors exhibit potent growth-suppressive activity in pancreatic and breast cancer cells. Cancer Res 2010;70:2445–2454.
31 Korangy F, Höchst B, Manns MP, Greten TF: Immune responses in hepatocellular carcinoma. Dig Dis 2010;28:150–154.
32 Kuang DM, Peng C, Zhao Q, Wu Y, Chen MS, Zheng L: Activated monocytes in peritumoral stroma of hepatocellular carcinoma promote expansion of memory T helper 17 cells. Hepatology 2010;51:154–164.
33 Kortylewski M, Xin H, Kujawski M, Lee H, Liu Y, Harris T, Drake C, Pardoll D, Yu H: Regulation of the IL-23 and IL-23 balance by Stat3 signaling in the tumor microenvironment. Cancer Cell 2009;15:114–123.
34 Kuang DM, Zhao Q, Peng C, Xu J, Zhang JP, Wu C, Zheng L: Activated monocytes in peritumoral stroma of hepatocellular carcinoma foster immune privilege and disease progression through PD-L1. J Exp Med 2009;206:1327–1337.
35 Wu K, Kryczek I, Chen L, Zou W, Welling TH: Kupffer cell suppression of CD8+ T cells in human hepatocellular carcinoma is mediated by B7-H1/programmed death-1 interactions. Cancer Res 2009;69:8067–8075.
36 Niemand C, Nimmesgern A, Haan S, Fischer P, Schaper F, Rossaint R, Heinrich PC, Müller-Newen G: Activation of STAT3 by IL-6 and IL-10 in primary human macrophages is differentially modulated by suppressor of cytokine signaling 3. J Immunol 2003;170:3263–3272.
37 Avella DM, Li G, Schell TD, Liu D, Zhang SS, Lou X, Berg A, Kimchi ET, Tagaram HR, Yang Q, Shereef S, Garcia LS, Kester M, Isom HC, Rountree CB, Staveley-O'Carroll KF: Regression of established hepatocellular carcinoma is induced by chemoimmunotherapy in an orthotopic murine model. Hepatology 2012;55:141–152.
38 Zhang W, Zhu XD, Sun HC, Xiong YQ, Zhuang PY, Xu HX, Kong LQ, Wang L, Wu WZ, Tang ZY: Depletion of tumor-associated macrophages enhances the effect of sorafenib in metastatic liver cancer models by antimetastatic and antiangiogenic effects. Clin Cancer Res 2010;16:3420–3430.
39 Luo Y, Zhou H, Krueger J, Kaplan C, Lee SH, Dolman C, Markowitz D, Wu W, Liu C, Reisfeld RA, Xiang R: Targeting tumor-associated macrophages as a novel strategy against breast cancer. J Clin Invest 2006;116:2132–2141.
40 Huang Y, Snuderl M, Jain RK: Polarization of tumor-associated macrophages: a novel strategy for vascular normalization and antitumor immunity. Cancer Cell 2011;19:1–2.
41 Wu WY, Li J, Wu ZS, Zhang CL, Meng XL: STAT3 activation in monocytes accelerates liver cancer progression. BMC Cancer 2011;11:506.

JJCO Japanese Journal of Clinical Oncology

Original Articles

Jpn J Clin Oncol 2012;42(4)256–263
doi:10.1093/jjco/hys001
Advance Access Publication 9 February 2012

High Expression of MicroRNA-210 is an Independent Factor Indicating a Poor Prognosis in Japanese Triple-negative Breast Cancer Patients

Tatsuya Toyama[1,*], Naoto Kondo[1], Yumi Endo[1], Hiroshi Sugiura[1], Nobuyasu Yoshimoto[1], Mai Iwasa[1], Satoru Takahashi[2,3], Yoshitaka Fujii[1] and Hiroko Yamashita[1]

[1]Department of Oncology, Immunology and Surgery, Nagoya City University Graduate School of Medical Sciences, 1 Kawasumi, Mizuho-cho, Mizuho-ku, [2]Department of Experimental Pathology and Tumor Biology, Nagoya City University Graduate School of Medical Sciences, 1 Kawasumi, Mizuho-cho, Mizuho-ku and [3]Division of Pathology, Nagoya City University Hospital, 1 Kawasumi, Mizuho-cho, Mizuho-ku, Nagoya 467-8601, Japan

*For reprints and all correspondence: Tatsuya Toyama, Department of Oncology, Immunology and Surgery, Nagoya City University Graduate School of Medical Sciences, 1 Kawasumi, Mizuho-cho, Mizuho-ku, Nagoya 467-8601, Japan. E-mail: toyamat-ncu@umin.ac.jp

Received September 29, 2011; accepted January 3, 2012

Objective: MicroRNAs have emerged as a new class of non-coding genes involved in regulating cell proliferation, differentiation and viability. Recent studies have identified miR-210 as one of a set of hypoxia-regulated microRNAs and demonstrated a direct regulatory role of HIF-1 alpha for its transcription. Here, we assessed miR-210 expression in Japanese triple-negative breast cancers and determined its clinical significance.

Methods: TaqMan MicroRNA assays for miR-210 expression were performed on 161 samples of Japanese breast cancer tissue (58 triple-negative breast cancer and 103 estrogen receptor positive/HER2 negative). Correlations between miR-210 expression and clinicopathological factors were analyzed. The effects of several variables on survival were tested by a Cox proportional hazards regression analysis.

Results: miR-210 expression in triple-negative breast cancers was significantly higher than in estrogen receptor-positive/HER2-negative breast cancers ($P < 0.001$). Patients whose triple-negative breast cancers showed low miR-210 expression experienced significantly better disease-free and overall survival than those with high miR-210 expression ($P = 0.02$ and $P = 0.05$, respectively). Although the prognosis of patients with triple-negative breast cancers is poor, Cox univariate and multivariate analyses demonstrated that a higher expression of miR-210 was an independent factor indicating a worse prognosis than for patients with a low level of miR-210.

Conclusions: The degree of miR-210 expression might be a clinically useful prognostic factor for decision-making regarding treatment in the adjuvant setting, especially in node-negative triple-negative breast cancer patients.

Key words: microRNA – miR-210 – breast cancer – triple negative

INTRODUCTION

MicroRNAs (miRNAs) have emerged as a new class of non-coding genes involved in regulating cell proliferation, differentiation and viability (1). miRNAs are single-strand small RNA molecules that are between 19 and 22 nucleotides in length. miRNAs primarily regulate gene expression through the inhibition of RNA translation by base pairing of their 'seed region', nucleotides 2–8, to the 3′ untranslated region of the target RNAs (2). miRNA can also facilitate targeting of specific mRNAs for cleavage, resulting in the down-regulation of target mRNAs (3).

Hypoxia is a common feature of pathological conditions such as tissue ischemia and inflammation, as well as solid tumors (4). Multiple hypoxic responses that impact tumorigenesis are mediated through the hypoxia-inducible factors (HIFs), composed of alpha (HIF-α) and beta (HIF-β; ARNT) subunits (4). Under hypoxia, HIF-α subunits are stabilized and heterodimerize with HIF-β in the nucleus. This heterodimeric complex binds to hypoxia response elements (HREs) and modulates the expression of multiple target genes that are important for angiogenesis, cell survival and tumorigenesis. Two HIF-α proteins, HIF-1α and HIF-2α regulate the expression of overlapping and unique target genes (4). In addition to the transcriptional activation of multiple genes, hypoxia is also involved in the regulation of miRNAs (5).

Several studies have reported that miR-210 is a highly up-regulated miRNA in hypoxic cells and have demonstrated its importance for cell survival (6–8). miR-210 was shown to be HIF-1α dependent and to have a functional role during tumor initiation (7). A recent study showed that HIF-1α could be a predominant and sufficient regulator of miR-210; however, in the presence of HIF-1α, HIF-2α could also mediate miR-210 expression (8). In addition to being one of the predominant hypoxia-inducible miRNAs, the expression of miR-210 is reported to be up-regulated in many cancers including breast (9,10), non-small-cell lung (11), head and neck (12) and pancreatic cancers (13), glioblastoma (14), malignant melanoma (8,15) and renal cell carcinoma (16). Overexpression of miR-210 was shown to indicate a poor prognosis in breast cancer patients (9,10), head and neck (12) and pancreatic cancer patients (13). miR-210 was also shown to be overexpressed at late stages of non-small-cell lung cancer (11).

Emerging data demonstrate that stratification of tumors by gene expression profiles divides breast cancer into four common subtypes that are associated with different clinical outcomes (17). Two of them are estrogen receptor (ER) positive (luminal and luminal/HER2+) and two are ER negative (basal-like and HER2 positive) (17,18). Although the immunohistochemical staining profile can be a useful surrogate for gene expression analysis, the optimal immunohistochemical profile of the basal-like subtype remains unclear. However, the basal-like category is composed almost entirely of triple-negative breast cancers (TNBCs; tumors lacking ER, progesterone receptor (PgR) and HER2 expression) (18,19). A simplified method of classification, based on immunohistochemical assays for ER, PgR and HER2, is clinically useful, and clinicians are increasingly taking triple-negative status into account in clinical decision-making and therapeutic protocol design. Triple-negative and basal-like tumors account for about 10–15% of all invasive breast cancers, and they usually have higher histological grades and more aggressive clinical behavior than hormone receptor-positive breast cancers (20,21).

In this study, we investigated the correlations between miR-210 expression, and clinicopathological parameters and prognosis in Japanese TNBC patients.

METHODS

Patients

A total of 161 surgically resected breast carcinomas with tissues available were selected from the archive of the Department of Breast and Endocrine Surgery, Nagoya City University Hospital in Japan. Specimens were obtained from patients who underwent surgery between January 1996 and July 2007. Tissues were fixed in 10% buffered formalin and embedded in paraffin and/or placed in liquid nitrogen immediately after resection and stored at −80°C until RNA extraction. Informed consent was obtained before the surgery. The histological grade was estimated according to the Bloom and Richardson method proposed by Elston and Ellis (22). Disease-free survival (DFS) was defined as the interval from the date of primary surgery to the earliest occurrence of one of the following: locoregional recurrence, distant metastasis or death from any cause. Overall survival (OS) was defined as the interval from the date of primary surgery to death from any cause. The median follow-up period was 5.4 years (range 3–149 months). This protocol was approved by the Institutional Review Board of Nagoya City University Graduate School of Medical Sciences and conformed to the guidelines of the 1975 Declaration of Helsinki.

Quantitative Reverse Transcription-PCR Detection of miRNA and mRNA

Total RNA from homogeneous microscopically confirmed breast cancer tissue was isolated from ~500 mg of each frozen specimen with TRIZOL reagent (Invitrogen Japan K.K., Tokyo, Japan) for RNA extraction according to the manufacturer's recommendations as described previously (21). cDNA was reverse transcribed from total RNA samples using specific miRNA primers from the TaqMan MicroRNA Assays and reagents from the TaqMan MicroRNA Reverse Transcription kit (Applied Biosystems, Foster City, CA, USA). The resulting cDNA was amplified by PCR using TaqMan MicroRNA Assay primers with the TaqMan Universal PCR Master Mix and analyzed with a 7500 ABI